CRYSTAL PLASTICITY MODELING OF SINGLE CRYSTAL Nb*

A. Mapar, D. Kang, T. R. Bieler[#], F. Pourboghrat, Michigan State University, East Lansing, MI 48824, USA

C. C. Compton, Facility for Rare Isotope Beams, East Lansing, MI 48824, USA

Abstract

Deformation behavior of niobium (Nb) is not thoroughly studied, although it is heavily used for superconducting applications. This deficiency of knowledge makes use of fine grain sheets desirable because they are easier to deform uniformly than anisotropic large grain sheets. Simulation models for deformation of Nb are limited. Therefore, design of a new manufacturing procedure is costly because models predicting the deformation of Nb are inaccurate.

Tensile tests were performed on single crystals with different orientations, to study the deformation behavior of Nb. Several crystal plasticity models were developed, calibrated and used to predict the deformation of single crystal tensile samples. This study compares the predictions of these models. As polycrystals are aggregates of single crystals, the model will also be useful for polycrystals.

INTRODUCTION

High-gradient SRF cavities are key enabling devices for high energy and high intensity science. Over the last decade the best cavities have achieved performance close to the theoretical limit (50 MV/m), but it has been challenging to fabricate cavities with reproducible properties and reproducible high performance. An increasing number of cavities are made from large-grain ($\geq$ ~5-10 mm, low GB density), high purity (RRR $\geq$ 200) niobium (Nb) slices, which have often shown superior properties to similarly processed cavities made from polycrystalline sheet metal with ~50 μm grain size, notably higher quality factors (Q). There is still variability in cavity performance that limits the ability to build accelerator cavities that consistently achieve accelerating gradients above 35 MV/m, which is not understood. Until the origins of this variability are understood and brought under control, (or at least detectable at an early stage of fabrication), the ability to build next generation accelerators capable of detecting phenomena comparable to the convincing evidence for the Higgs Boson in 2012 [1], may not be achieved at an acceptable cost.

Mechanical cavity shape fabrication by traditional deep drawing, hydroforming, or other deformation history affects cavity performance. Defect structures that develop during deformation include dislocations, sub-structures with low and high angle boundaries, and altering the character of initial grain boundaries (GBs). These all influence the performance of surface chemical and thermal treatments on the cavity during the fabrication process.
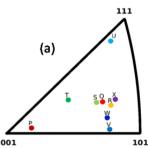
This study is a continuation of [2] that was presented at SRF 2013, which along with [3], provides more details on development of the crystal plasticity model and experimental procedures.

CRYSTAL PLASTICITY CONSTITUTIVE MODEL DEVELOPMENT

Unlike continuum based finite element constitutive models that are in common use in finite element codes, crystal plasticity models simulate the physical slip processes that take place in a particular grain orientation in response to an imposed stress (or strain). Constitutive model development that is capable of simulating the stress-strain behavior of Nb single crystals is challenging, requiring novel approaches motivated by physical understanding to develop suitable hardening rules.

The inverse pole figure in Fig. 1a shows the orientation of the tensile axis nine single crystal tensile samples. Fig. 1b shows the stress-strain behavior of these samples. The long nearly flat flow stress evolution in many of the orientation near the center of the inverse pole figure triangle implies that very little dislocation accumulation took place, i.e. dislocations enter and
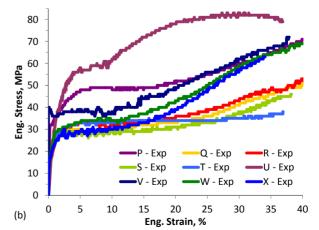

Figure 1: (a) The tensile axis of samples used in this study. (b) Stress-strain response of annealed single crystal samples.

leave from opposite surfaces of the single crystal at about the same rate. With rotation of the crystal resulting from dominant slip on one system, secondary slip systems gradually become more favorable, and their activation leads to gradually increasing dislocation density, as dislocations moving in different directions interact and create barriers that stimulate dislocation multiplication and further interactions that increase the hardening rate. The Dynamic Hardening Model, in equation (1), captures this behavior:

$$\dot{\tau}_{Dy}^{\alpha} = \sum_{\beta=1}^{N} h^{\alpha\beta} \left|\dot{\gamma}^{\beta}\right| \left((1-w) + w\left(\frac{\gamma^{2nd}}{\gamma^{1st}}\right)^{n}\right) \quad (1)$$

This effect is accomplished with a ratio of shear on the second to the first most active slip system $\gamma^{2nd}/\gamma^{1st}$ that is small until the secondary slip process is more similarly activated. The hardening rate leads to an increase in the shear stress $\dot{\tau}^{\alpha}$ needed to deform the next increment of shear strain $\dot{\gamma}^{\beta}$ on each of the β slip systems according to the hardening function $h^{\alpha\beta}$ where the hardening relationship between slip systems is considered. The Dynamic hardening exponent n adjusts the hardening rate. A weighting factor w allows the dynamic hardening effect to be moderated, which recognizes the fact that an initial sample has pre-existing dislocations that do interfere with the primary slip system. This model reduces to the classical hardening model when $w = 0$.

Classical hardening laws observed in polycrystals show power law hardening, e.g. similar to a square root relationship with downward curvature, leading to gradually decreasing hardening rates. However, many of these samples show upward curvature, implying gradual development of hardening mechanisms. Note that the upward curvature occurs sooner with orientations that are closer to the edge of the triangle, as less rotation is needed before the orientation reaches the edge or corner, where 2 or more slip systems have equal driving force. Hence an exponentially increasing hardening rule is needed to capture this effect.

To obtain the exponential features of the hardening observed experimentally, h^{β} in the classical hardening model [2,3] is modified. This modification is denoted with h_{DE}^{β} and has the following definition:

$$h_{DE}^{\beta} = \left[h_{stage\,1}^{\beta} - h_{stage\,2}^{\beta}\right] \cdot < k_{\tau} - \frac{Max(\tau^{\beta})}{\tau_{s}} > \cdot$$

$$< k_{\gamma} - \frac{\gamma^{2nd}}{\gamma^{1st}} > + h_{stage\,2}^{\beta} \quad (2)$$

$$h_{stage\,1}^{\beta} = h_{0} \left|1 - \frac{\tau_{c}^{\beta}}{\tau_{s}}\right|^{a} \cdot sgn\left(1 - \frac{\tau_{c}^{\beta}}{\tau_{s}}\right) \quad (3)$$

$$h_{stage\,2}^{\beta} = h_{0} exp[(1 + \gamma^{1st})^{q} + \gamma^{1st}] \quad (4)$$

where k_{τ} and k_{γ} are material constants, $h_{stage\,1}^{\beta}$ and $h_{stage\,2}^{\beta}$ define the hardening rate of the first and second stage of the deformation of a single crystal. Equation (2) is called the Differential-Exponential (DE) hardening model and defines a criteria for prediction of the onset of second stage of deformation. Finally, this model defines the hardening model the materials as:

$$\dot{\tau}_{y}^{\alpha} = \sum_{\beta=1}^{N} h_{DE}^{\beta} \left[q + (1-q)\delta^{\alpha\beta}\right] \left|\dot{\gamma}^{\beta}\right| \quad (5)$$

Where q is a material constant and $\delta^{\alpha\beta}$ is the Kronecker delta. When the crystal plasticity model with the above hardening rule is calibrated the overall flow behavior of different orientations is more effectively simulated up to the point where the exponential hardening process becomes important. This approach is novel, and has not been introduced before. This modification, here referred to as the "Differential-Exponential" model uses two separate definitions to predict the first and second stage of deformation of single crystals. The hardening rate of the first stage is simulated with the classical hardening model. The rate of hardening of the second stage is modeled as the exponential function of the shear strain on the most active slip system. A criterion is devised to predict the onset of the second stage of the hardening and switch form the classical model to the exponential model.

There are additional approaches for dealing with intrinsic anisotropy in BCC metals that involve more complex rules that account for the fact that BCC metals do not follow the Schmid law consistently. This is due to the fact that for a screw dislocation to move, more information is needed than just the resolved shear stress acting on the slip system, i.e. the critical resolved shear stress is a sensitive function of the details of the stress tensor that affect how constriction of the relaxation of a screw dislocation on different planes that contain the Burgers vector (screw dislocation line direction) occurs [4,5]. This is known as the non-Schmid model.

A non-Schmid yield and a flow potential is developed for Nb and implemented in the crystal plasticity model.

CALIBRATING THE MODEL

Nine single crystal tensile dog-bone samples with different crystal orientations were cut from a Nb slice. The samples were annealed at 800°C for two hours before being monotonically deformed to 40% engineering strain. More details on sample preparation and experiments are given in [6]. The details of Figure 1a shows the orientation of tensile axis of these samples with respect to the crystal orientation.

The Dynamic Hardening model and the non-Schmid models were each simultaneously calibrated with the stress-strain curves of sample P and T. The calibration process includes finding a meaningful set of material parameters that fit the predictions of the model to the results of the experiments. The Differential-Exponential model was calibrated with the sample P and R. Commercial optimization software LS-OPT was used for calibration. For details of this process are explained in [7].

Figures 2, 3 and 4 show the calibration of the Dynamic hardening, non-Schmid and Differential-Exponential models against the engineering stress - engineering strain response of samples P, T. and R. Figure 3 also shows the

predictions of the Differential-Exponential model and Figure 4 includes the predictions of the Dynamic and non-Schmid models.

Sample T shows a single slip behavior, while sample R shows the second stage of the hardening. Since the Dynamic hardening model and the non-Schmid model do not have the tools to predict the change of the hardening rate, they were calibrated to P and T. The Differential-Exponential model was calibrated to P and R so that the change of the hardening rate is captured by the material parameters.

The calibrated models were used to predict the deformation behavior of the seven other single crystal samples. Figures 5-10 show the predictions of the models for the rest of the tensile samples.

DISCUSSION

Figures 2-10 illustrate how the Dynamic and Differential-Exponential models are becoming able to simulate experiments realistically. The dynamic hardening rule suppresses the rate of hardening until a secondary slip direction is sufficiently activated to create barriers that lead to dislocation multiplication. Previous studies [2,3] showed the classical hardening, when calibrated to P and T similar to the Dynamic hardening or non-Schmid model, is not able to predict the flow behavior of other samples. This recognizes that predominant single slip does not lead to much hardening.

Predictions of the non-Schmid crystal plasticity model are similar to the Dynamic hardening model, except this
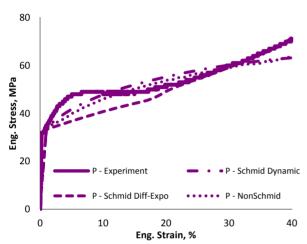
Figure 2: Sample P was used to calibrate all models. Each model was simultaneously calibrated to two experiments. The Dynamic hardening and the non-Schmid models were calibrated with P and T and the Differential-Exponential model was calibrated with P and R.

Figure 4: Sample R was used to calibrate the Differential-Exponential model, simultaneously with sample P. This figure also shows the predictions of the Dynamic hardening and the non-Schmid models for sample T.
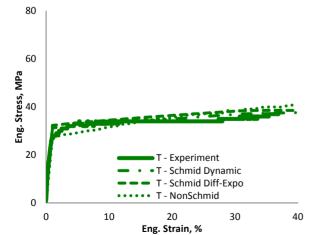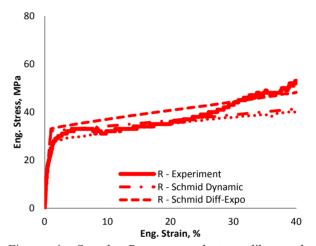
Figure 3: Sample T was used to calibrate the Dynamic hardening and the non-Schmid models, simultaneously with sample P. This figure also shows the prediction of the Differential-Exponential model for sample T.
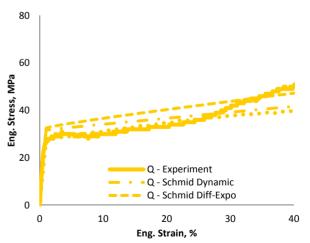
Figure 5: Comparing predictions of the models with the experiment of Q. Predictions of the Dynamic hardening and non-Schmid models are close. The Differential-Exponential model predicts single slip behavior for this sample.
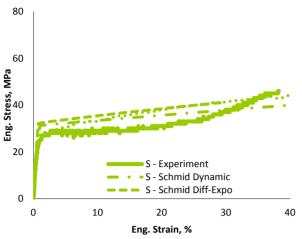
Figure 6: Comparing predictions of the models with the experiment of S. Predictions of the Dynamic hardening and non-Schmid models are close. The Differential-Exponential model predicts single slip behavior for this sample.

Figure 8: Comparing predictions of the models with the experiment of V. Predictions of the Dynamic hardening and non-Schmid models are close. The Differential-Exponential model predicts a two-stage behavior for this sample.
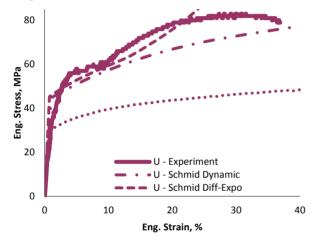

Figure 7: Comparing predictions of the models with the experiment of U. Prediction of the Dynamic hardening model is close to the experiment. The non-Schmid model fail for this sample. The Differential-Exponential model predicts a two-stage behavior for this sample.

Figure 9: Comparing predictions of the models with the experiment of W. Predictions of the Dynamic hardening and non-Schmid models are close. The Differential-Exponential model predicts a two-stage behavior for this sample.

non-Schmid model fails for sample U. The closeness of the predictions of these two models suggest that although it is a BCC metal, the non-Schmid effects are small for Nb.

The Differential-Exponential model effectively predicts the stress-strain behavior of Nb. From figures 2-10 it is evident that using a two-stage hardening rule improves the predictions of the crystal plasticity model. The model predicts single slip for Q, R, S and T and duplex slip P, U, V, W and X, which matches well with the experiments.

CONCLUSION

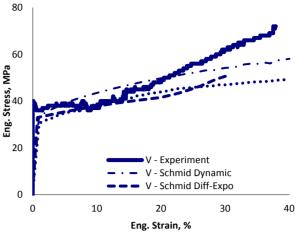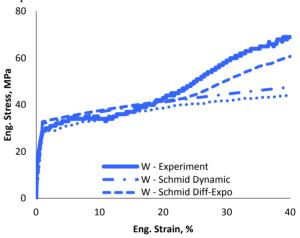The models presented in this paper improve the accuracy of the classical crystal plasticity model. The Dynamic Hardening model is a method to decrease the hardening rate at the beginning of the deformation and increase it as the deformation goes on. This method improves the predictions of the crystal plasticity model, although it cannot account for the abrupt change of the hardening rate which happens when the second stage of the deformation starts. The Differential-Exponential model was devised to address this shortcoming. This model defines two separate hardening equations of for stage I and II of deformation of single crystals and a criterion to switch between these two equations. This model effectively predicts the stress-strain behavior of Nb single crystal up to 40% engineering strain. The predictions of the Dynamic hardening model, on the other hand are more accurate in smaller strains.

Some BCC materials show considerable sensitivity to components of the stress tensor that cause stresses other than the Schmid resolved shear stress. The level of sensitivity and the effective stress components change with the material [8,9]. A non-Schmid crystal plasticity model developed to study the non-Schmid behavior of Nb. The predictions of this model are similar to the Dynamic hardening model, nevertheless the non-Schmid model fail for sample U. This suggests the sensitivity of Nb to the non-Schmid stresses is small however, further studies are needed to prove this point.
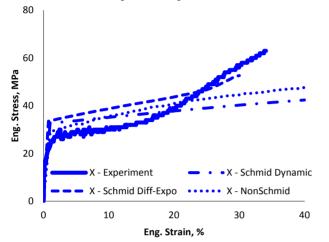

Figure 10: Comparing predictions of the models with the experiment of X. Predictions of the Dynamic hardening and non-Schmid models are close. The Differential-Exponential model predicts a two-stage behavior for this sample.

REFERENCES

[1] Aad G, et al, L. Phys Lett Sect B Nucl Elem Part High-Energy Phys 2012;716:1.

[2] Mapar A, Bieler TR, Pourboghrat F, Compton C. Dynamic Hardening Rule; a Generalization of the Classical Hardening Rule for Crystal Plasticity, in:. 16th Int. Conf. RF Supercond. Paris, France: 2013.

[3] Mapar A, Bieler TR, Pourboghrat F, Compton CC. Crystal Plasticity Finite Element Modeling of Single Crystal Niobium Tensile Tests with Weighted Dynamic Hardening Rule, in:. Li M, Campbell C, Thornton K, Holm E, Gumbsch P (Eds.). 2nd World Congr. Integr. Comput. Mater. Eng. TMS (The Minerals, Metals & Materials Society); 2013.

[4] Qin Q, Bassani JL. 1992;40:835.

[5] Qin Q, Bassani JL. 1992;40:813.

[6] Kang D, Baars DC, Mapar A, Bieler TR, Pourboghrat F, Compton CC. Study of Slip and Deformation in High Purity Single Crystal Nb for Accelerator Cavities, in:. This Proceeding. 2015.

[7] Stander N, Basudhar A, Basu U, Gandikota I, Savic V, Sun X, Choi KS, Hu X, Pourboghrat F, Park T, Mapar A, Kumar S, Ghassemi-Armaki H, Abu-Farha F. Multi-Scale Material Parameter Identification Using LS-DYNA® and LS-OPT®, in:. 10th Eur. LS-DYNA Conf. Würzburg, Germany: DYNAmore GmbH; 2015.

[8] Gröger R, Vitek V. Acta Mater 2008;56:5426.

[9] Gröger R, Bailey AG, Vitek V. Acta Mater 2008;56:5401.